Applied Catalysis B: Environmental 91 (2009) 180–188

Contents lists available at ScienceDirect

Applied Catalysis B: Environmental

journal homepage: www.elsevier.com/locate/apcatb

Wet air oxidation with tubular ceramic membranes modified with polyelectrolyte/Pt nanoparticle films☆

David M. Dotzauer [a], Ali Abusaloua [b], Sylvain Miachon [b,1], Jean-Alain Dalmon [b], Merlin L. Bruening [a,*]

[a] Department of Chemistry, Michigan State University, East Lansing, MI 48824, United States
[b] Institut de Recherches sur la Catalyse et l'Environnement de Lyon, UMR 5256 CNRS/Université Claude Bernard Lyon 1, 69626 Villeurbanne, France

ARTICLE INFO

Article history:
Received 26 February 2009
Received in revised form 12 May 2009
Accepted 18 May 2009
Available online 27 May 2009

Keywords:
Catalysis
Layer-by-layer
Membrane
Wet air oxidation

ABSTRACT

Gas–liquid reactions with membrane-supported catalysts often use the interfacial contactor configuration in which the reaction occurs at the gas–liquid-catalyst interface within the membrane. Thus, control over the catalyst location in the membrane is crucial for making efficient use of expensive materials such as noble metal nanoparticles. Layer-by-layer (LBL) adsorption of polyelectrolyte/metal nanoparticle films in tubular ceramic membranes allows deposition of the catalytic nanoparticles only near the interior of the tube, where the gas–liquid interface is typically located. In wet air oxidation of formic acid, tubular membranes modified by LBL deposition of polyelectrolyte/Pt nanoparticle films show 2 to 3 times higher specific activities than similar membranes modified by traditional methods such as anionic impregnation/reduction and evaporation/recrystallization/reduction. In acetic acid and phenol oxidations, the LBL method gives order of magnitude increases in specific activity relative to the traditional membrane modification methods. The enhanced activity with LBL-modified membranes is likely due to the controlled deposition of the Pt in the catalytic inner layer of the tubes, as only the LBL method gives tubular membranes that show higher activity than pulverized membranes in stirred tank reactors.

1. Introduction

Wet air oxidation is an important process in which hazardous organic pollutants react with oxygen to give more benign compounds, ideally H_2O and CO_2 [1–3]. This technique is attractive for processing wastewater pollutants that are too dilute to be treated by incineration [4,5] and too concentrated to be treated by biological methods [6–9]. Traditional wet air oxidation of organic and inorganic substrates often requires high temperature and pressure (150–350 °C, 20–200 bar air) [10,11], but the use of catalysts such as Pt, Ru, or other precious metals immobilized on inorganic powders allows much milder reaction conditions (room temperature, 1–5 bar air) [12–14]. However, implementation of catalytic wet air oxidation in conventional stirred tank reactors requires a catalyst recovery step, and reaction rates are often limited by diffusion of oxygen and/or the liquid phase compounds to the catalyst surface.

Porous membranes are an attractive alternative to powders as catalyst supports because the high internal surface area of the membrane affords a high loading of the active catalyst material, and there is no need to separate the catalyst from the reaction mixture. Thus, reactions can run continuously. Furthermore, catalytic membranes operated as gas–liquid contactors enhance the accessibility of the reactants to the metal catalyst [15]. The two most common membrane configurations for gas–liquid reactions are flow-through and interfacial contactors. Flow-through contactors, where all reactants flow through the membrane in a single solution, are advantageous because when the membrane pores are sufficiently small, reactions will not be limited by the rate of mass transport to the catalyst [16]. Furthermore, by controlling the flow rate and, hence, the residence time of a substrate within the membrane, side reactions may be minimized to give high selectivity for a particular product [17–21]. Unfortunately, in gas–liquid reactions with flow-through contactors the low solubility of the gaseous reactant in the liquid phase often limits the extent of reaction [16]. A similar problem occurs in fixed-bed reactors. In interfacial contactors, the walls of a catalytic membrane serve as the interface between gas and liquid phases (Fig. 1) to allow rapid transport of gas to the solid–liquid-catalyst interface and provide a high catalytic activity [22]. Recent work by Pera-Titus et al. also suggests that the enhanced catalytic activity

☆ We dedicate this article to our friend and remarkable colleague Sylvain Miachon.

* Corresponding author. Tel.: +1 517 355 9715x237; fax: +1 517 353 1793.
E-mail address: bruening@chemistry.msu.edu (M.L. Bruening).

[1] Deceased on January 21, 2009.

0926-3373/$ – see front matter © 2009 Elsevier B.V. All rights reserved.
doi:10.1016/j.apcatb.2009.05.022

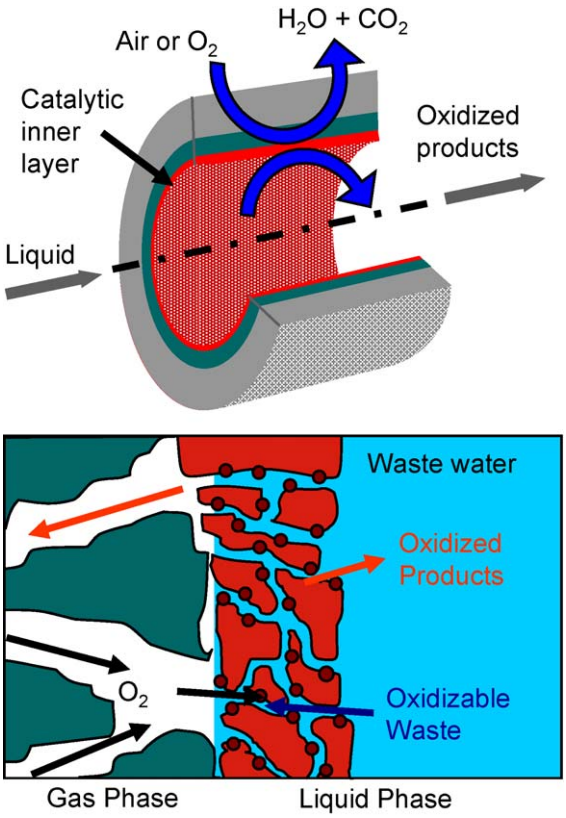

Fig. 1. Schematic diagram showing the interfacial contactor configuration in a tubular membrane and its application to wet air oxidation.

in interfacial contactors may be due to increased gas solubility in the confined pores of the membrane [23]. However, if pore sizes are larger than 10 nm, this effect is not observed.

A number of studies in the Watercatox project examined the use of tubular catalytic membranes as interfacial contactor reactors for wet air oxidation of model and industrial effluents at the laboratory and pilot scale [24–29]. These studies showed that the interfacial contactor configuration leads to increased activity when compared to a conventional stirred tank reactor, and that the high activity stems from the ability to control the location of the gas–liquid interface within the membrane (Fig. 1). In the interfacial contactors thus far employed for wet air oxidation, catalytic noble metal particles were formed in the membrane by evaporation/recrystallization/reduction and anion impregnation/reduction methods [30,31], but other strategies for particle deposition may provide even higher catalytic activities.

Among the many methods for incorporating precious metal catalysts in porous materials [32–37], layer-by-layer (LBL) adsorption of polyelectrolyte/metal nanoparticle films is attractive because it offers fine control over nanoparticle size and composition and can be applied to a variety of membrane materials [38]. LBL adsorption of complementary materials has been investigated by many groups for modification of flat surfaces [39–41], and when charged nanoparticles are utilized as one of the alternating layers, careful selection of adsorption conditions sometimes allows immobilization of well-separated nanoparticles with control over the amount of material deposited [42,43]. One requirement of any technique used for catalyst deposition in interfacial contactors is that the precious metal catalysts are highly concentrated in the membrane region where the gas/liquid interface occurs. Because LBL nanoparticle adsorption in membranes is very rapid, the depth to which deposited nanoparticles penetrate the membrane can be readily controlled by limiting the amount of nanoparticle-containing solution passed through the membrane. Hence it is a simple matter to localize catalyst deposition in the inner layer of a tubular membrane.

This research examines wet air oxidation of formic acid, acetic acid, and phenol using tubular ceramic membrane modified with Pt nanoparticles by LBL deposition. Results from these membranes are compared with data from membranes modified by conventional techniques used in the Watercatox project. The LBL-modified membranes have especially high specific activities (activities normalized to Pt content) in the oxidation of these model compounds.

2. Experimental methods

Anodisc aluminum oxide membranes (25 mm disks with 0.2 or 0.1 μm diameter pore sizes, Whatman), tubular ceramic membranes (Pall Exekia) and 100 mesh aluminum oxide (Aldrich) were modified with catalytic nanoparticles using the LBL technique. The tubular membranes (25 cm long, 7 mm inner diameter, 10 mm outer diameter) consisted of three layers: a TiO_2-covered alumina support layer with 12 μm-diameter pores, a TiO_2-covered alumina intermediate layer with 0.8 μm-diameter pores, and a ZrO_2 inner layer with 50 nm-diameter pores. Hexachloroplatinic acid, potassium tetrachloroplatinate(II), mercaptosuccinic acid, sodium citrate, sodium borohydride, poly(acrylic acid) (PAA, Mw = 5000), poly(-allylamine hydrochloride) (PAH, Mw = 17,000), and branched poly(ethylenimine) (PEI, Mw = 25,000) were obtained from Aldrich.

2.1. Modification of aluminum oxide powder

LBL modification of the alumina powder involved: (1) stirring 2.5 g of alumina powder in 20 mL of PAA solution (0.02 M PAA, 0.5 M NaCl, pH adjusted to 4.5 with 1 M NaOH) for 10 min; (2) stirring the PAA-modified powder in 20 mL of PAH solution (0.02 M PAH, 0.5 M NaCl, pH adjusted to 5.0 with 0.1 M HCl) for 10 min; and (3) stirring the PAA/PAH-coated powder in 20 mL of a metal nanoparticle solution for 10 min. (Polymer concentrations are given with respect to the repeating unit.) After each of the above steps, the liquid was decanted, and the alumina powder was washed three times with 20 mL of deionized water. Pt nanoparticles were prepared with thiol or citrate stabilizing agents. To synthesize the thiol-stabilized particles, under vigorous stirring 5 mL of 0.0676 M $NaBH_4$ was added to an aqueous solution containing 10 mL of 3.38 mM $H_2PtCl_6{\cdot}6H_2O$ and 1 mL of 0.0237 M mercaptosuccinic acid (MSA) [44]. The resulting MSA-stabilized Pt solution was diluted by a factor of 4 prior to use in LBL adsorption. To prepare the citrate-stabilized particles, 30 mL of a 1 wt% aqueous sodium citrate solution was added to 255 mL of a refluxing solution of 0.3 mM $H_2PtCl_6{\cdot}6H_2O$ under vigorous stirring. The solution was refluxed for 4 h to allow completion of the reaction [45]. The resulting Pt nanoparticle solution was used directly for deposition on the alumina powder. Alumina powder (2.5 g) was also modified by the anionic impregnation technique by stirring the powder in a 0.1 g/L solution of H_2PtCl_6 for 2 h, washing three times with 20 mL of deionized water, reducing the Pt ions to nanoparticles by adding 20 mL of 0.1 M $NaBH_4$ and stirring for 10 min, and rinsing three more times with 20 mL of deionized water. The Pt content of modified alumina powder samples was determined by dissolving the Pt with aqua regia and analyzing the solutions with atomic absorption spectroscopy (AAS). The amounts of Pt in the three catalysts were 0.82, 0.56, and 0.44 mg Pt per g powder for anionic impregnation, MSA-stabilized, and citrate-stabilized samples, respectively.

2.2. Membrane modification

LBL modification of disk-shaped alumina membranes was described previously for membranes containing polyelectrolyte/

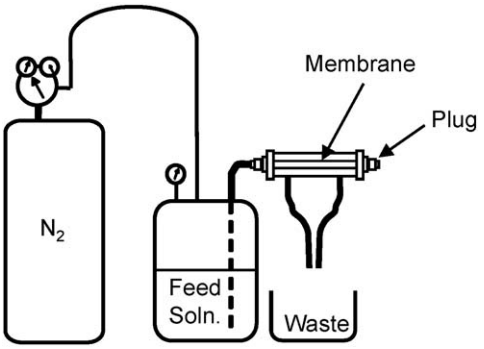

Fig. 2. Schematic diagram of the apparatus used for depositing polyelectrolyte/metal nanoparticle films in tubular ceramic membranes. The pressurized solution flows through the membrane pores in an inside-out configuration.

Au nanoparticle films [46]. Briefly, deposition of each layer involved passing the polyelectrolyte or nanoparticle solution through the membrane using a peristaltic pump located at the permeate side of the membrane. For these membranes, the films consisted of an initial PAA layer followed by a PAH/metal nanoparticle bilayer. The as-prepared Pt nanoparticle solutions were diluted by a factor of 4 prior to deposition in the alumina membranes. As described in detail below, tubular ceramic membranes were modified by several variations of the LBL method as well as by the evaporation/crystallization/reduction and anionic impregnation/reduction techniques. During LBL modification, polyelectrolyte and metal nanoparticle solutions were deposited by flowing from the inside of the membrane to the outside as shown in Fig. 2.

2.2.1. Method 1—LBL with ex situ nanoparticle formation $[PAA/PAH/Pt\text{-}NP]_1$

For tubular membranes, the modification procedure included sequential flow through the membrane of 250 mL of PAA solution (0.002 M PAA, 0.1 M NaCl, pH adjusted to 4.5), 500 mL of water, 250 mL of PAH solution (0.002 M PAH, 0.1 M NaCl, pH adjusted to 5), 500 mL of water, 1000 mL of a citrate-stabilized Pt nanoparticle solution prepared by diluting 25 mL of as-prepared colloid solution with 975 mL of water, and 500 mL of water. The flow rate of the solutions through the membrane was between 20 and 25 mL/min and was maintained by applying a pressure between 0.2 and 0.5 bar. Fig. 3-1 shows a general scheme of this procedure.

2.2.2. Method 2—LBL with in situ nanoparticle formation $[PAA/PEI\text{-}Pt(0)]_1$

In a slight modification to previous procedures for modifying alumina powder with polyelectrolyte/Pd nanoparticle films [47], method 2 incorporated a PEI–Pt complex in the deposition procedure rather than preformed Pt nanoparticles. Briefly modification included sequential flow through the membrane of 250 mL of PAA solution (0.002 M PAA, 0.1 M NaCl, pH adjusted to 4.5), 500 mL of water, and 250 mL of PEI solution that contained Pt(II) (0.002 M PEI, 0.0004 M K_2PtCl_4, pH adjusted to 9). To form Pt nanoparticles, 250 mL of 0.1 M $NaBH_4$ was passed through the membrane to reduce the Pt salt (Fig. 3-2), and the membrane was rinsed by the passage of 500 mL of water.

2.2.3. Method 3—LBL with in situ nanoparticle formation $[Pt(0)/PEI]_2$

Similar to a previous method for modifying alumina powder [48], the membrane was first immersed in a solution of chloroplatinic acid (0.1 g Pt/L) for 20 h so that the inside and outside of the tube were in contact with solution. After putting the membrane in the holder, 500 mL of water was passed through the membrane pores to remove excess Pt solution. PEI was deposited by flowing 250 mL of solution (0.002 M, 0.1 M NaCl, pH adjusted to 9) through the membrane, which was subsequently rinsed by passage of 500 mL of water. A second $PtCl_6^{2-}$/PEI bilayer was deposited similarly before reducing the Pt with $NaBH_4$ in the same manner as in method 2 (Fig. 3-3).

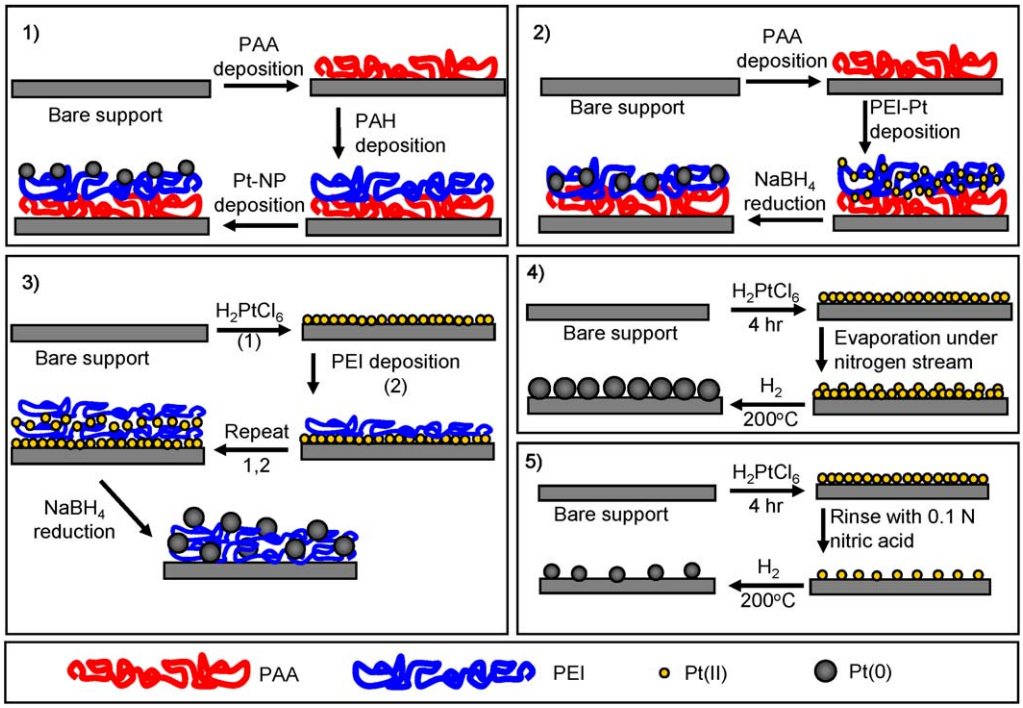

Fig. 3. Schematic diagram of modification of membrane pore surfaces using (1) layer-by-layer deposition of PAA/PAH/Pt-nanoparticle films, (2) layer-by-layer deposition of PAA/PEI–Pt(II) films followed by reduction, (3) layer-by-layer deposition of $[Pt(II)/PEI]_2$ films followed by reduction, (4) evaporation/recrystallization of H_2PtCl_6 followed by reduction, and (5) anionic impregnation with H_2PtCl_6 followed by reduction.

2.2.4. Method 4—evaporation/recrystallization with reduction by hydrogen at 200 °C

The technique of evaporation/recrystallization was similar to a previously reported procedure in the Watercatox project [30]. Briefly, the membrane was immersed in a 0.1 g/L chloroplatinic acid solution for 4 h, removed from the solution, and allowed to dry at room temperature. Evaporation of the solvent led to concentration of the Pt precursor on the surface of the membrane with more of the Pt located in the inner layer. Reduction of the Pt was performed by placing the membrane under flowing H_2 at 200 °C (Fig. 3-4).

2.2.5. Method 5—anionic impregnation with reduction by hydrogen at 200 °C

The anionic impregnation technique was also performed in a manner similar to previous Watercatox research [30]. In this case, the support was immersed in a 0.1 g/L chloroplatinic acid solution for 4 h and then rinsed by flowing a 0.1 N nitric acid solution through the pores to remove any unbound Pt species from the membrane. After rinsing with water and then drying under flowing nitrogen at 100 °C, the Pt was reduced under flowing hydrogen at 200 °C (Fig. 3-5).

2.3. Characterization

Nanoparticle solutions were characterized by transmission electron microscopy (TEM) to determine the approximate size and shape of the nanoparticles, and TEM was also used to demonstrate the deposition of nanoparticle-containing films in disk-shaped porous alumina membranes. Prior to imaging, the membrane was ground into a powder with a mortar and pestle and dispersed in water using a vortex mixer. A drop of the resulting solution was then placed onto a carbon-coated copper grid and dried before analysis. The Pt content of the disk-shaped membranes was determined by completely leaching the metal with aqua regia (3 parts HCl, 1 part HNO_3) and analyzing the leachate by flame AAS. For tubular membranes, the amount of deposited Pt was estimated by AAS analysis of the deposition solutions before and after passing them through the membrane. These values were verified by grinding the membranes into powder with a mortar and pestle, dissolving the Pt in aqua regia, and analyzing the solution by AAS.

2.4. Catalytic reactions

Formic acid, acetic acid, and phenol were employed as substrates for oxidation reactions. Initial experiments were performed with powder catalysts to see if the nanoparticle stabilizer or deposition technique affected the nanoparticle activity. In these reactions, oxygen was continuously bubbled into 50 mL of a vigorously stirred solution containing catalyst and 5 g/L of formic acid. Samples of the reaction mixture were collected after several time intervals and analyzed by ion chromatography (Dionex LC20, Ionpac AS16 column) to determine the amount of formic acid that remained in solution. Similar experiments were also performed with powders prepared by grinding tubular membranes.

Reactions performed with disk-shaped membranes were carried out by continuously bubbling oxygen into a formic acid solution and then passing that solution through a nanoparticle-modified membrane at a given flux. Samples of the membrane effluent were analyzed by ion chromatography to determine the extent of formic acid oxidation.

For interfacial contactor reactions, the modified tubular membranes were mounted in a gas tight module that allows the flow of liquid through the lumen of the tube and countercurrent gas flow on the shell side of the tube (Fig. 4). The liquid flow rate was typically between 7 and 10 mL/min, and the gas overpressure was set to values between 0.2 and 4 bar. The gas flow rate was maintained at 50 mL/min with a mass flow controller. Air was used as the oxidant in all of the interfacial contactor reactions, which were carried out at 20 or ~60 °C by controlling the temperature of the feed solution. The starting concentrations of formic acid, acetic acid, and phenol were 5 g/L (0.108 M), 3.25 g/L (0.054 M), and 1.7 g/L (0.018 M), respectively, and correspond to carbon contents of approximately 1.3 g/L in each case. For the interfacial contactor reactions, the conversion of each substrate was monitored using total organic carbon (Shimadzu TOC 5050A) and/or HPLC (Varian Prostar with UV–vis detection) analysis. The uncertainty in the calculated specific activities was <10% for formic acid oxidation experiments and <20% for acetic acid and phenol oxidation experiments.

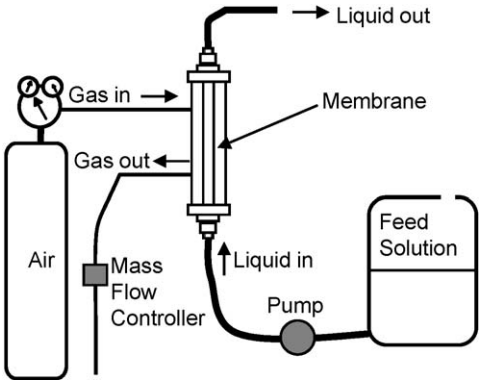

Fig. 4. Schematic diagram of the wet air oxidation apparatus that employs tubular catalytic membranes as interfacial contactors.

3. Results and discussion

3.1. Membrane characterization

TEM images of nanoparticles and membrane samples were collected to determine the size and shape of the Pt nanoparticles and to see if these particles are effectively deposited in the membranes. The images and size distributions of MSA- and citrate-stabilized Pt nanoparticles in Fig. 5 show that the average particle diameters are 2.6 and 3.2 nm, respectively. Fig. 6 presents TEM images of the citrate-stabilized Pt nanoparticles immobilized in a disk-shaped alumina membrane by method 1 (Fig. 3). These images show that LBL deposition yields a high density of nanoparticles within the pores of the membrane and that there is minimal particle aggregation, which should lead to accessible nanoparticles with a high catalytic surface area.

The amount of Pt in each of the tubular membranes was determined by chemical analysis of precursor Pt solutions before and after passing them through the membrane. These values were later confirmed by dissolving the immobilized Pt in aqua regia and analyzing these solutions by AAS. Table 1 shows that the two methods for determining the amount of immobilized Pt are in good agreement for all membranes except those prepared by method 5. The difference in the two values for method 5 is likely due to some Pt being washed away in the nitric acid rinsing step during the membrane modification. This Pt loss is not accounted for in the initial mass balance. For all membranes, the Pt content is 200–1000 mg of Pt per m^2 (1–5 mg of Pt per membrane), based on the area calculated from the inner tube diameter, and the relatively similar Pt loading among the different membranes facilitates comparison of their catalytic activities.

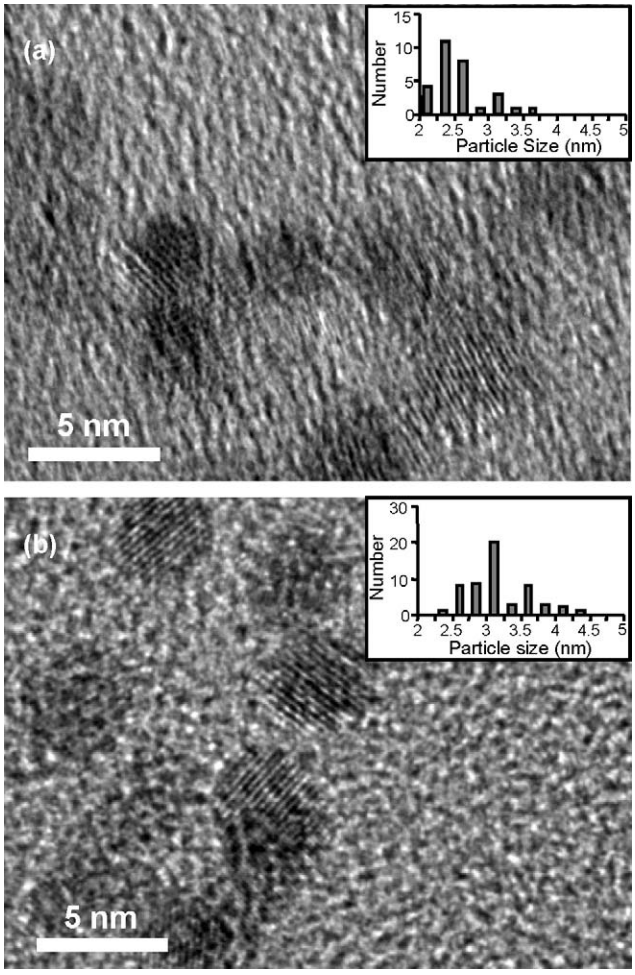

Fig. 5. TEM images of (a) mercaptosuccinic acid-stabilized Pt nanoparticles and (b) citrate-stabilized Pt nanoparticles on carbon-coated copper grids. The inset in each image shows the nanoparticle size distribution determined from several high resolution TEM images.

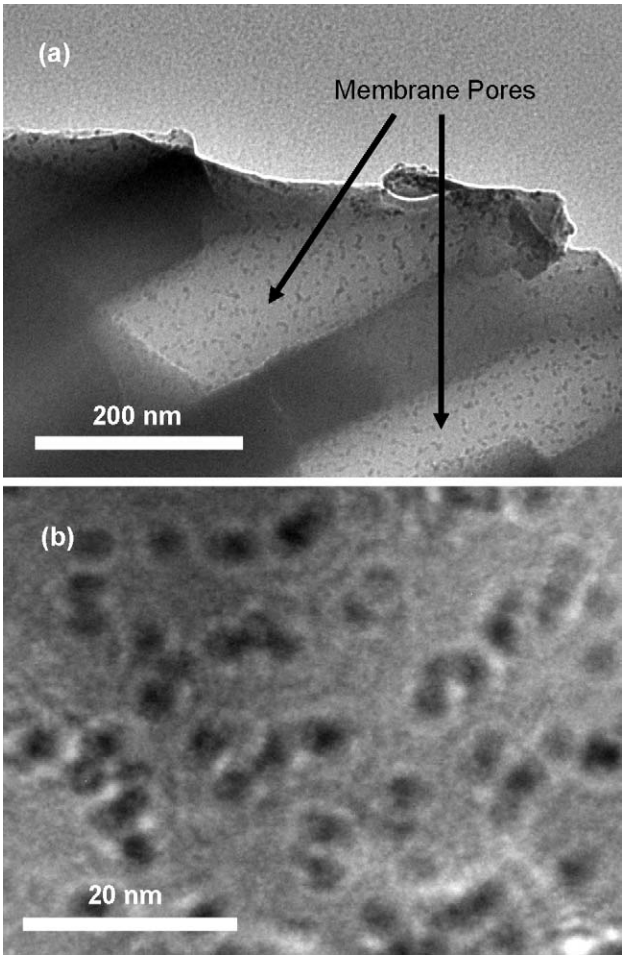

Fig. 6. Low (a) and high (b) magnification TEM images of pores of an alumina membrane modified with a PAA/PAH/Pt nanoparticle film. The Pt nanoparticles contained in the film are citrate-stabilized.

3.2. Wet air oxidation catalyzed by Pt nanoparticles on alumina powder

To examine the effect of the stabilizing agent on the activity of Pt nanoparticles, alumina powder was modified with a PAA/PAH bilayer and either citrate- or MSA-stabilized Pt nanoparticles to prepare heterogeneous catalysts. In wet air oxidation of formic acid with these materials, the catalyst modified with citrate-stabilized Pt nanoparticles exhibits an activity of 1.3 ± 0.2 mmol/(s gPt) whereas the catalyst containing MSA-stabilized Pt nanoparticles has an activity of 0.7 ± 0.1 mmol/(s gPt). The average nanoparticle size is similar for both types of particles, so differences in surface area should not account for the difference in activity. In fact, of the two types of nanoparticles, MSA-stabilized particles show slightly smaller diameters (higher surface area per mass) in TEM images (Fig. 5). The most likely explanation for the difference between the two types of nanoparticles is that the thiol stabilizers bind more tightly than citrate to the surface of the nanoparticle, and this stronger binding limits the number of active sites for catalysis. Previous studies of catalysis by thiol-stabilized metal nanoparticles also reported low reaction rates [49,50]. Alumina powder modified by impregnation of $PtCl_6^{2-}$ and subsequent reduction of Pt(IV) to Pt nanoparticles shows an activity of 1.0 ± 0.1 mmol/(s gPt), which is again lower than that of the catalyst containing citrate-stabilized nanoparticles. Thus, LBL deposition with citrate-stabilized nanoparticles provides catalysts with comparable or better activities than traditional methods of catalyst preparation. Furthermore, these data suggest that the polyelectrolyte multilayer does not inhibit the activity of the Pt nanoparticles.

3.3. Oxidation of formic acid in disk-shaped membranes

In initial studies of membrane-based oxidation, solutions sparged with O_2 were passed through an alumina membrane coated with a PAA/PAH/Pt nanoparticle film. Fig. 7 shows the results of these studies. At initial formic acid concentrations <2 mM, nearly all of the formic acid is oxidized to CO_2 and water

Table 1
Pt contents in tubular membranes.

Modification method	Pt loading (mg Pt/m^2)[a]	
	Mass balance[b]	Membrane powder[c]
1	220 ± 40	220 ± 20
2	220 ± 20	200 ± 20
3	910 ± 90	830 ± 80
4	470 ± 60	480 ± 40
5	690 ± 90	400 ± 40

[a] Based on an internal membrane surface area of 0.00506 m^2 (internal tube diameter of 7 mm, active length of 230 mm).
[b] Determined by chemical analysis of precursor solutions before and after deposition.
[c] Determined by chemical analysis of aqua regia solutions used to remove Pt from ground membrane samples.

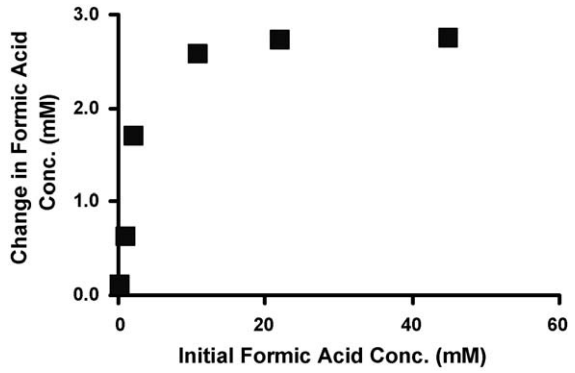

Fig. 7. Change in formic acid concentration in membrane-catalyzed oxidation with several initial formic acid concentrations. (The membrane acted as a flow-through contactor.) Solutions were sparged with O_2, and the flux through the disk-shaped porous alumina membrane modified with citrate-stabilized Pt nanoparticles (method 1) was 0.023 mL/(cm^2 s).

during passage through the membrane because at these concentrations, formic acid is the limiting reactant. However, at formic acid concentrations >10 mM, the amount of oxidation is essentially independent of initial formic acid concentration because O_2 is the limiting reagent. The solubility of O_2 in water at 1 atm of O_2 is roughly 1.25 mM [51], which would correspond to a concentration of 2.5 mM formic acid that could be oxidized. This is similar to the maximum change in formic acid concentration seen in Fig. 7.

For oxygen-sparged solutions containing 10.8 mM formic acid, increasing the solution flux through the membrane did not significantly affect decreases in formic acid concentration (Fig. 8). This again suggests that the reaction is limited by the amount of O_2 in the solution because if the reaction were kinetically limited, we would expect smaller declines in the formic acid concentration at higher flow rates due to lower residence times in the membrane. In most fast gas–liquid reactions with flow-through contactors, the solubility of the gas in solution will limit the reaction rate unless high gas pressures are employed. For this reason, tubular interfacial contactors are often more attractive than flow-through contactors for membrane-catalyzed gas–liquid reactions such as wet air oxidation.

3.4. Wet air oxidation with tubular membranes

This section compares the catalytic activities of five types of tubular interfacial contactor membranes (Fig. 3) in sequential studies of the oxidation of formic acid, acetic acid, and phenol.

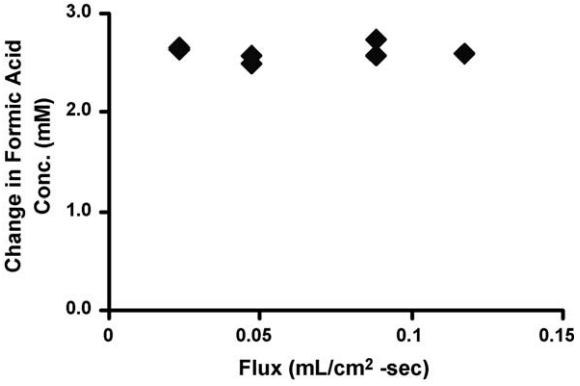

Fig. 8. Change in formic acid concentration during membrane-catalyzed oxidation as a function of flux through a nanoparticle-modified disk-shaped alumina membrane (method 1). (The membrane acted as a flow-through contactor.) The initial solution concentration was 10.8 mM and solutions were sparged with O_2 before passing through the membrane.

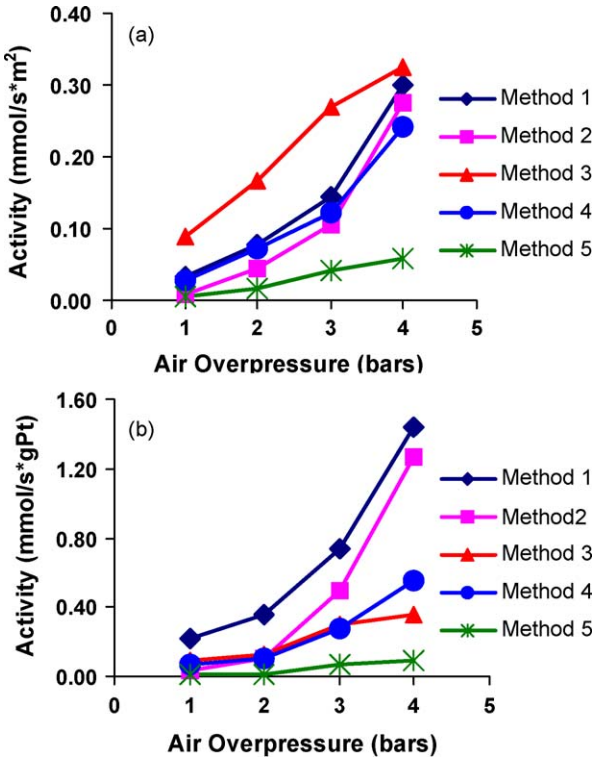

Fig. 9. Normalized rate of formic acid oxidation vs. air overpressure for Pt-containing membranes prepared by the methods shown in Fig. 3. (The membrane served as an interfacial contactor.) Normalization was performed with respect to (a) the area of the internal wall of the membrane and (b) the amount of Pt in the membrane.

Experiments were performed on at least two membranes modified by each method. Because catalyst deactivation often occurs during phenol oxidation [52], membranes were again tested in the oxidation of formic acid after experiments with phenol to see if catalyst deactivation occurred.

3.4.1. Formic acid oxidation

Initially, formic acid oxidation was examined at 1, 2, 3, 4, and 4.3 bar of air overpressure to determine the effect of overpressure on reaction rates (Fig. 9). High air overpressures increase the solubility of O_2 in the solution, but more importantly, they control the location of the gas–liquid interface. The highest activity in formic acid oxidation occurs at 4 or 4.3 bar of overpressure because the gas–liquid interface is closest to the inner layer of the tube where most of the catalyst is located. However, in some cases much of the air begins to come through the defects in the membrane at an overpressure of 4.3 bar. As a result, the catalytic activity sometimes starts to decrease at 4.3 bar because the gas/liquid interface is no longer well-maintained in the catalytic layer of the membrane. This is consistent with previous results [28].

Membranes prepared by methods 1 and 2 exhibit similar rates of formic acid oxidation and similar specific activities (Fig. 9). Membranes prepared by method 3 show a similarly high reaction rate (Fig. 9a), but because the platinum content of these membranes is higher than that of all other membranes (Table 1), their specific activity at overpressures >3 bar is lower than for membranes prepared by methods 1 and 2 (Fig. 9b). This is not surprising because in method 3, the initial Pt deposition occurs throughout the membrane, not just in the surface layer. Only the Pt that is near the gas–liquid interface is efficiently used for formic acid oxidation. In Fig. 9a, the relatively high oxidation rates at low overpressures for the membranes prepared by method 3 likely

occur because at low overpressures the gas–liquid interface is deeper in the tube wall, where these particular membranes still have significant amounts of Pt.

Membranes prepared by method 4 show a high rate of formic acid oxidation (Fig. 9a) but a lower activity per gram of Pt (Fig. 9b) than methods 1 and 2. This suggests that method 4 deposits the platinum deeper into the membrane than methods 1 and 2, and therefore the specific activity with method 4 membranes is low at the higher air overpressures because all of the platinum is not being used effectively. On the other hand, the membranes prepared by method 5 exhibit a much lower activity than those prepared by the other four methods. This is expected because $PtCl_6^{2-}$ does not bind well to the surface of ZrO_2 and is easily removed during the nitric acid rinsing step. Therefore, the Pt is mostly bound to regions that are not washed well with nitric acid. Since these regions most likely appear away from the gas–liquid interface, the method 5 membranes should have relatively low activity.

When comparing the LBL-modified membranes (methods 1–3) with membranes described in the literature, the rate per membrane area is only 1/3 to 1/2 as high as published values [29]. On the other hand, the rate is ~5-fold higher than published values when normalizing to Pt content. The specific activity is also ~50% higher than previous values obtained with "low-loading" membranes, which had Pt contents similar to the membranes prepared in this study [29].

3.4.2. Acetic acid oxidation

Similar to results with formic acid, the rate of acetic acid oxidation at room temperature is highest at 4 or 4.3 bar (Fig. 10). The oxidation rate was determined by TOC analysis and thus tells how much of the acetic acid is completely oxidized to CO_2 and H_2O but does not account for any partial conversion to formic acid.

Fig. 10a shows that membranes prepared by methods 1 and 2 have a much higher activity for room temperature acetic acid oxidation than membranes prepared by the other 3 methods. The membranes prepared by method 3 show a small specific activity, but membranes prepared by methods 4 and 5 exhibit essentially no detectable activity for acetic acid oxidation at room temperature. At 60 °C, membranes prepared by methods 1–4 exhibit higher activity than at room temperature, as expected. In the case of membranes prepared by methods 1 and 2, on going from room temperature to 60 °C, the activity increases by about 60% and 90%, respectively. In contrast, the activities of membranes prepared by methods 3 and 4 increase by factors of 9 and 10, respectively. Even with this large increase in activity, however, the membranes prepared by methods 3 and 4 still have a lower activity at 60 °C than the membranes prepared by the first two methods. The membranes prepared by method 5 show low activity even at the higher temperature.

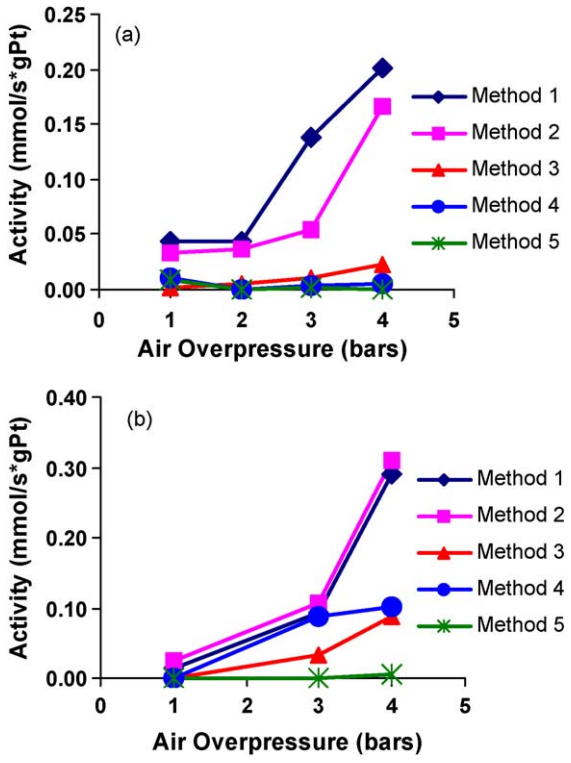

Fig. 10. Normalized rates of membrane-catalyzed acetic acid oxidation vs. air overpressure for different membrane types at (a) room temperature and (b) 60 °C. (The membrane served as an interfacial contactor.) Oxidation rates were normalized to the amount of Pt in the membrane.

3.4.3. Phenol oxidation

In phenol oxidation, samples were collected at 1, 3, and 4 bar overpressures and subsequently analyzed by both TOC and HPLC. In TOC analysis, catalytic activities are determined from the difference in carbon content between the inlet and outlet solutions, whereas in HPLC analysis, catalytic activities are determined from the decrease in phenol concentration. Similar to previous experiments involving oxidation of formic acid and acetic acid, the highest activity occurs at air overpressures of 4 bar.

Tables 2 and 3 show that, again, the highest activity occurs with membranes prepared by methods 1 and 2, and that membranes prepared by method 5 show little or no activity for the oxidation of phenol. Membranes prepared by methods 3 and 4 exhibit more than 4-fold lower specific activities than membranes prepared by the first two methods, even at higher temperature. Oxidation experiments performed at 60 °C result in higher activities (two times higher or more) than experiments performed at room temperature. We would expect to achieve even higher activities with temperatures in excess of 150 °C [14,52], but these high temperatures are not compatible with the experimental apparatus (Fig. 4) used in this study. Furthermore, these high temperatures may also lead to film deformation and possible sintering of the catalyst. Future studies need to explore the stability of polyelectrolyte/metal nanoparticle films at temperatures at or above 150 °C.

The catalytic activities determined from HPLC are generally higher than those from TOC because TOC analysis only shows how much of the sample is transformed to CO_2 or insoluble species, whereas HPLC shows how much phenol is oxidized to any product. The higher activities seen with HPLC suggest that some phenol is oxidized to smaller organic compounds, and not completely to CO_2. Because the conversion in phenol oxidation is low (<10%), the quantities of these other compounds in the analyzed samples are below detectable levels in HPLC. As a result, the identity and amount of each byproduct in the reaction were not determined. The activities determined by TOC analysis and HPLC are generally in better agreement at 60 °C than at room temperature, suggesting

Table 2
Catalytic activities of several tubular membranes in phenol oxidation at room temperature with 4 bar air overpressure.

Preparation method	Activity	
	[a]mmol/(s gPt)	[b]mmol/(s gPt)
1	0.064	0.13
2	0.050	0.11
3	0.006	0.015
4	0.000	0.000
5	0.003	0.012

[a] Determined by TOC analysis.
[b] Determined from HPLC analysis.

Table 3
Catalytic activities of several tubular membranes in phenol oxidation with a feed temperature of 60 °C with 4 bar air overpressure.

Preparation method	Activity	
	[a]mmol/(s gPt)	[b]mmol/(s gPt)
1	0.15	0.21
2	0.11	0.21
3	0.026	0.035
4	0.027	0.025
5	0.003	0.000

[a] Determined by TOC analysis.
[b] Determined from HPLC analysis.

Table 4
Catalytic activities in formic acid oxidation for tubular membranes used as interfacial contactors and as powders in conventional stirred tank reactors.

Modification method	Activity (mmol/s gPt)	
	Interfacial contactor[a]	Conventional reactor[b]
1	1.5 ± 0.3	0.6 ± 0.05
2	1.3 ± 0.2	0.5 ± 0.03
3	0.5 ± 0.1	0.7 ± 0.1
4	0.7 ± 0.2	0.5 ± 0.03
5	0.1 ± 0.03	0.5 ± 0.1

[a] Activity at air overpressure = 4 bar.
[b] Pure O_2 was sparged into the reaction mixture.

that more of the phenol is converted to CO_2 and H_2O at higher temperatures.

After phenol oxidation, the various membranes were again used to catalyze formic acid oxidation at room temperature to determine if the oxidation of refractory compounds like phenol causes catalyst deactivation. While a decrease in activity for formic acid oxidation could be due to poisoning or other effects such as nanoparticle leaching or aggregation, a constant activity may suggest that the extent of catalyst deactivation is minimal. However, if formic acid oxidation is simply limited by O_2 solubility, then catalyst deactivation would not be observed by this method. In nearly all cases, there was no decrease in formic acid oxidation rates after using the membranes for phenol oxidation. However, one of the membranes prepared by method 4 showed a 40% activity decrease in formic acid oxidation after the membrane was used for phenol oxidation. The decreased activity may have been due to leaching of Pt for that specific membrane or to poisoning of the catalyst during phenol oxidation. With that exception, each membrane maintained a constant activity for formic acid oxidation.

3.4.4. Conventional reactions with pulverized tubular membranes

To show that the interfacial contactor configuration is advantageous for these reactions, each type of membrane was also ground into a powder that was used as a heterogeneous catalyst in a conventional stirred tank reaction. In these reactions, a solution containing 0.108 M formic acid was continuously bubbled with oxygen while stirring rapidly. Pure oxygen was used as the oxidant instead of air to provide as much oxygen to the reaction as possible. The results in Table 4 show that all five types of membranes in the powder form have similar activities when normalized to the amount of Pt in the catalyst. However, the activities of different membranes operated as interfacial contactors vary significantly with the method of modification. In the case of methods 1 and 2, membranes operated as interfacial contactors at 4 bar overpressure show activities that are ~2.5 times higher than those of membrane powders used as heterogeneous catalysts. Conversely, membranes prepared by methods 3 and 4 exhibit little difference in activity between interfacial contactors and powder catalysts, and the membrane prepared by method 5 shows higher activity in the conventional reaction. These results demonstrate that the interfacial contactor configuration can be quite valuable for gas–liquid reactions, but to take full advantage of this configuration, the catalyst must be localized in the inner layer of the membrane.

4. Conclusions

The overall objective of this study was to compare the catalytic activity of membranes prepared using LBL deposition methods with the activity of membranes prepared by the traditional methods of evaporation/recrystallization/reduction and anionic impregnation/reduction. Although the rate of formic acid oxidation with LBL-modified membranes was 1/3 to 1/2 lower than previous results when normalized to membrane surface area, the rate when normalized to Pt content improved ~5-fold. In this study, the Pt content for all membranes studied was less than 5 mg of Pt per membrane.

Membranes prepared by LBL methods 1 and 2 exhibited the highest activity when normalized to the Pt content inside the membranes, most likely because of strong localization of the Pt in the inner layer of the tubular membrane. Conversely, the other three methods deposit Pt on the entire surface of the membrane, which means that any Pt that gets deposited on the support layer or intermediate layer is most likely not being utilized when performing oxidation at higher air overpressures.

The biggest limitation to the methods involving LBL deposition is the low loading of Pt. Since the support is quite expensive, the cost of Pt is not as much of a concern as in other systems; however, Pt cost cannot be disregarded. In the future, low loading with the LBL method can be overcome by optimizing the LBL deposition procedure or by depositing multiple layers. Further studies should also include examination of catalytic activity in continuous experiments over longer periods of time to learn more about the catalyst stability. (Experiments in this study were typically performed only for a few hours.) LBL modification is quite versatile and could also be applied to polymeric hollow fiber supports, which are much less expensive than the traditional ceramic supports. This should result in a more cost-effective system for gas–liquid reactions as long as the polymer membrane is sufficiently stable.

Acknowledgement

We thank the National Science Foundation (OIS 0530174) for funding this research.

References

[1] V.S. Mishra, V.V. Mahajani, J.B. Joshi, Ind. Eng. Chem. Res. 34 (1995) 2–48.
[2] F.J. Zimmerman, Chem. Eng. 65 (1958) 117–120.
[3] F. Luck, Catal. Today 53 (1999) 81–91.
[4] E. Guibelin, Water Sci. Technol. 49 (2004) 209–216.
[5] B.J. Kim, S. Qi, R.S. Shanley, Water Environ. Res. 66 (1994) 440–455.
[6] P. Adriaens, T.M. Vogel, in: L.Y. Young, C.E. Cerniglia (Eds.), Microbial Transformation and Degradation of Toxic Organic Chemicals, Wiley, New York, 1995, pp. 435–486.
[7] C.A. Fewson, Trends Biotechnol. 6 (1988) 148–153.
[8] Y.I. Matatov-Meytal, M. Sheintuch, Ind. Eng. Chem. Res. 37 (1998) 309–326.
[9] M. Jeworski, E. Heinzle, Biotechnol. Annu. Rev. 6 (2000) 163–196.
[10] H. Debellefontaine, J.N. Foussard, Waste Manage. (Oxford) 20 (2000) 15–25.
[11] F. Luck, Catal. Today 27 (1996) 195–202.
[12] J. Levec, A. Pintar, Catal. Today 124 (2007) 172–184.
[13] D. Pham Minh, P. Gallezot, S. Azabou, S. Sayadi, M. Besson, Appl. Catal. B 84 (2008) 749–757.
[14] A. Pintar, J. Batista, T. Tisler, Appl. Catal. B 84 (2008) 30–41.
[15] A. Julbe, D. Farrusseng, C. Guizard, J. Membr. Sci. 181 (2001) 3–20.
[16] R. Dittmeyer, K. Svajda, M. Reif, Top. Catal. 29 (2004) 3–27.
[17] G. Bengtson, D. Fritsch, Desalination 200 (2006) 666–667.

[18] H. Purnama, P. Kurr, A. Schmidt, R. Schomäcker, I. Voigt, A. Wolf, R. Warsitz, AlChE J. 52 (2006) 2805–2811.
[19] A. Schmidt, R. Haidar, R. Schomäcker, Catal. Today 104 (2005) 305–312.
[20] A. Schmidt, R. Schomäcker, J. Mol. Catal. A: Chem. 271 (2007) 192–199.
[21] C. Lange, S. Storck, B. Tesche, W.F. Maier, J. Catal. 175 (1998) 280–293.
[22] M. Reif, R. Dittmeyer, Catal. Today 82 (2003) 3–14.
[23] M. Pera-Titus, S. Miachon, J.-A. Dalmon, AlChE J. 55 (2009) 434–441.
[24] S. Miachon, V. Perez, G. Crehan, E. Torp, H. Raeder, R. Bredesen, J.A. Dalmon, Catal. Today 82 (2003) 75–81.
[25] H. Raeder, R. Bredesen, G. Crehan, S. Miachon, J.-A. Dalmon, A. Pintar, J. Levec, E.G. Torp, Sep. Purif. Technol. 32 (2003) 349–355.
[26] E.E. Iojoiu, S. Miachon, E. Landrivon, J.C. Walmsley, H. Raeder, J.-A. Dalmon, Appl. Catal. B 69 (2007) 196–206.
[27] E.E. Iojoiu, E. Landrivon, H. Raeder, E.G. Torp, S. Miachon, J.-A. Dalmon, Catal. Today 118 (2006) 246–252.
[28] E.E. Iojoiu, J.C. Walmsley, H. Raeder, S. Miachon, J.-A. Dalmon, Catal. Today 104 (2005) 329–335.
[29] E.E. Iojoiu, S. Miachon, J.-A. Dalmon, Top. Catal. 33 (2005) 135–139.
[30] D. Uzio, S. Miachon, J.-A. Dalmon, Catal. Today 82 (2003) 67–74.
[31] V. Perez, S. Miachon, J.-A. Dalmon, R. Bredesen, G. Pettersen, H. Raeder, C. Simon, Sep. Purif. Technol. 25 (2001) 33–38.
[32] P. Braunstein, H.-P. Kormann, W. Meyer-Zaika, R. Pugin, G. Schmid, Chem. Eur. J. 6 (2000) 4637–4646.
[33] K. Daub, V.K. Wunder, R. Dittmeyer, Catal. Today 67 (2001) 257–272.
[34] C. Perego, P. Villa, Catal. Today 34 (1997) 281–305.
[35] G. Centi, R. Dittmeyer, S. Perathoner, M. Reif, Catal. Today 79–80 (2003) 139–149.
[36] L. Gröschel, R. Haidar, A. Beyer, H. Coelfen, B. Frank, R. Schomäcker, Ind. Eng. Chem. Res. 44 (2005) 9064–9070.
[37] J. Xu, A. Dozier, D. Bhattacharyya, J. Nanopart. Res. 7 (2005) 449–467.
[38] D.M. Dotzauer, J. Dai, L. Sun, M.L. Bruening, Nano Lett. 6 (2006) 2268–2272.
[39] J. Schmitt, G. Decher, W.J. Dressick, S.L. Brandow, R.E. Geer, R. Shashidhar, J.M. Calvert, Adv. Mater. 9 (1997) 61–65.
[40] T.C. Wang, M.F. Rubner, R.E. Cohen, Chem. Mater. 15 (2003) 299–304.
[41] J. Dai, M.L. Bruening, Nano Lett. 2 (2002) 497–501.
[42] D. Lee, M.F. Rubner, R.E. Cohen, Nano Lett. 6 (2006) 2305–2312.
[43] J.W. Ostrander, A.A. Mamedov, N.A. Kotov, J. Am. Chem. Soc. 123 (2001) 1101–1110.
[44] S. Chen, K. Kimura, J. Phys. Chem. B 105 (2001) 5397–5403.
[45] P.A. Brugger, P. Cuendet, M. Graetzel, J. Am. Chem. Soc. 103 (1981) 2923–2927.
[46] D.M. Dotzauer, S. Bhattacharjee, Y. Wen, M.L. Bruening, Langmuir 25 (2009) 1865–1871.
[47] S. Bhattacharjee, M.L. Bruening, Langmuir 24 (2008) 2916–2920.
[48] S. Kidambi, M.L. Bruening, Chem. Mater. 17 (2005) 301–307.
[49] S.E. Eklund, D.E. Cliffel, Langmuir 20 (2004) 6012–6018.
[50] J. Alvarez, J. Liu, E. Roman, A.E. Kaifer, Chem. Commun. (2000) 1151–1152.
[51] F.D. Wilde (Ed.), Field Measurements: U.S. Geological Survey Techniques of Water-Resources Investigations, book 9, chap. A6, accessed from http://www.ubs.water.usgs.gov/twri9A/on2/6/2009.
[52] S. Nousir, S. Keav, Barbier Jr., M. Bensitel, R. Brahmi, D. Duprez, Appl. Catal. B 84 (2008) 723–731.